ELECTROMAGNETIC DIFFRACTION EFFICIENCIES FOR PLANE REFLECTION DIFFRACTION GRATINGS

A. S. Marathay
T. E. Shrode

Second Year
Final Report
Prepared for the
National Aeronautics and
Space Administration
Under Contract NAS5-11456

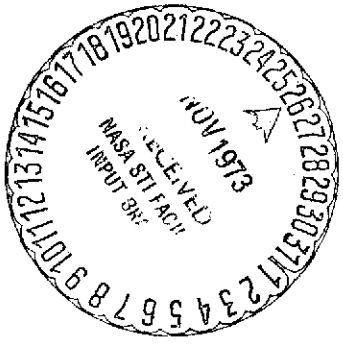

Optical Sciences Center
University of Arizona
Tucson, Arizona 85721
July 1973

ELECTROMAGNETIC DIFFRACTION EFFICIENCIES FOR PLANE REFLECTION DIFFRACTION GRATINGS

A. S. Marathay
T. E. Shrode

Second Year
Final Report
Prepared for the
National Aeronautics and
Space Administration
Under Contract NAS5-11456

Optical Sciences Center
University of Arizona
Tucson, Arizona 85721
July 1973

ABSTRACT

In this report we present the results of our research activities during the past year (FY 1972-1973) on holographic grating research. A large portion of this work was performed using rigorous vector diffraction theory; therefore, we have included the necessary theory in this report. The diffraction efficiency studies begun in the first year (FY 1971-1972) were continued using programs based on a rigorous theory. The simultaneous occurrence of high diffraction efficiencies and the phenomenon of double Wood's anomalies is demonstrated along with a graphic method for determining the necessary grating parameters. Also, an analytical solution for a grating profile that is perfectly blazed is obtained. The performance of the perfectly blazed grating profile is shown to be significantly better than grating profiles previously studied. Finally, we describe a proposed method for the analysis of coarse echelle gratings using rigorous vector diffraction that is currently being developed.

CONTENTS

1. INTRODUCTION

During the past two years our research activities have been directed at the analysis, design, and evaluation of diffraction gratings produced by holographic techniques. During the first year of this contract (1971-1972) we applied approximate equations, derived from vector diffraction theory, to the study of diffraction gratings with different groove profiles. In particular, we studied echelette profiles that have rounded edges. This profile is very similar to those produced using holographic methods. For these studies computer programs, based on the approximate theory, were developed and tested to determine their regions of validity. The programs were then used to study the efficiency characteristics to be expected from holographic gratings. We were able to show that holographic gratings can be designed so that nearly all of the incident radiant energy is contained in a preselected diffraction order for a particular wavelength. It was also shown that these high blaze efficiencies occur in the presence of a double Wood's anomaly.

During the following year of this contract (1972-1973) we continued the above studies. The earlier studies had shown that the computer programs based on the approximate theory worked very well for gratings with shallow grooves but that the approximations were not valid for gratings with deep grooves. To avoid a duplication of effort, we obtained a set of computer programs based on rigorous vector diffraction theory and valid for deep echelette gratings. These programs were made available by Professor A. R. Nereuther at the University of California, Berkeley. The programs are based on the works of Dr. K. A. E. H. Zaki[1] and Dr. H. A. Kalhor.[2] Throughout this report the results obtained from the use of these programs will be clearly distinguished from those obtained using our own programs.

The Berkeley programs were first modified so that they were easier to use. Also, an attempt was made to modify the programs so that they could analyze gratings with an arbitrary profile. However, this effort was not successful as the results obtained from the programs were no longer always reliable. Thus, the latter modifications were removed from the programs.

The study of the design of blazed diffraction gratings was extended to include an analytical solution to the problem. It was shown that it was possible to design a grating profile so that 100% of the incident energy was contained in a preselected diffraction order. In addition, the grating was now well blazed over a broad wavelength interval as opposed to a single wavelength as was obtained in the previous study mentioned earlier.

It became apparent, through close contact with our contract monitor and his associates, that the needs of NASA-GSFC far exceeded the capabilities of the programs based on the approximate theory as well as the Berkeley programs in their present form. This was primarily due to the very deep gratings and the large number of real diffraction orders resulting from coarse echelle gratings that were used in the vacuum ultraviolet. In order to analyze these gratings we directed all of our recent efforts toward the formulation of an efficient

method by which the equations derived from rigorous vector diffraction theory could be applied to the analysis of coarse echelle gratings as required by NASA. The salient features of the rigorous theory are discussed in the next section. In Section 5 we outline a method that can be used for the study of coarse echelle gratings. A more complete mathematical derivation of the equations required for the study is presented in Appendix B, C, and D.

2. VECTOR DIFFRACTION FROM DEEP GROOVE DIFFRACTION GRATINGS

The grooves in a diffraction grating are said to be deep when the groove depth approaches or is greater than the wavelength of the incident radiant energy. To analyze such a grating a rigorous theory that allows the amplitude coefficients of the diffracted fields to be a function of position within the grating profile must be used. It is apparent that the assumption that the amplitude coefficients are constant within the grating groove will become less valid as the grating depth increases. In fact, this is exactly why the approximate theory fails when used to analyze deep gratings. Below we describe a rigorous theory that can be applied to the analysis of deep echelle gratings.

Consider a perfectly conducting, planar reflection grating that is irradiated by a monochromatic plane wave. We wish to determine the amount of energy appearing in each of the diffracted orders. This is done by using Maxwell's electromagnetic field equations and applying the appropriate boundary conditions.

The total electromagnetic field is defined as the incident field plus the diffracted fields

$$\text{Total field} \equiv (\text{Incident field}) + (\text{Diffracted fields}).$$

This applies to both the electric field **E** as well as the magnetic field **H**. We assume a right-handed coordinate system such that the y axis is perpendicular to the plane of the grating, the x axis is perpendicular to the grating grooves, and the z axis is parallel with them. The grating profile is given by

$$y = f(x). \tag{1}$$

An electromagnetic wave with any arbitrary state of polarization can be decomposed into two waves linearly polarized at right angles to each other. Therefore, we consider two cases: In the first the electric field vector is parallel to the grating grooves and is called the E-parallel state of polarization. In the second the magnetic field vector is parallel to the grating grooves and is called the H-parallel state of polarization. This decomposition reduces the vector equations to scalar equations. On the surface of the grating the boundary conditions to be obeyed by each state of polarization are given by

(a) E-parallel

$$E_{\text{TOT}}(x,y)\Big|_{\substack{\tan \\ y = f(x)}} \equiv 0. \tag{2}$$

That is, the tangential component of the total electric field on the surface of the grating must be zero.

(b) H-parallel

$$\left.\frac{\partial H_{\mathrm{TOT}}(x,y)}{\partial n}\right|_{y=f(x)} \equiv 0. \tag{3}$$

which says that the normal derivative of the total magnetic field on the surface of the grating must be zero.

With the use of Maxwell's equations and the application of the above boundary conditions it is possible to calculate the desired diffraction efficiencies. Below we have briefly described the procedure used to perform this calculation. The procedure we describe is exactly the same as that used by Zaki and Kalhor.

The first step is to calculate the field due to an infinitely long alternating line current by using Maxwell's equations. This information is then used to determine the fields due to an infinite array of equally spaced line currents. The result of this calculation is then used to formulate a suitable Green's function that describes the problem. In formulating the Green's function the currents are assumed to be excited by a plane wave incident at an angle θ_i. The Green's function so obtained is a function of x,y and x',y' separately. That is, the Green's function describes the fields at the point x,y due to an infinite line current at the point x',y'. Due to the choice of the phasing of the individual line currents, the Green's function exhibits the following symmetry

$$G(x+ma,y;x'+pa,y') = \exp(-ikma\sin\theta_i)\, G(x,y;x',y') \tag{4}$$

where a is the grating constant and m and p are positive or negative integers. We note that for a normally incident plane wave ($\theta_i = 0$) the Green's function is strictly periodic in both variables x and x'.

Having obtained the Green's function we then use Green's identity to obtain the diffracted fields. The surface integral that appears in Green's identity is evaluated by considering the volume enclosed by the surfaces shown in Fig. 1. The surface S_1 is along the grating surface. The surfaces S_5 and S_6 (not shown in the figure) are parallel to the plane of the paper and are the front and rear surfaces of the closed volume. It can be shown that the contributions due to S_5 and S_6 are equal and opposite as are the contributions due to S_2 and S_3. The contribution due to the integration along S_4 can easily be determined. Therefore, we find that the field at any point within the volume that is enclosed by the different surfaces is given by the surface integral along the grating profile. For the E-parallel polarization we obtain

$$E_d(x',y') = \exp(+ikx'\sin\theta_i) \int_{S_1} G(x,y;x',y')\, \frac{\partial E(x,y)}{\partial n}\, dl \tag{5}$$

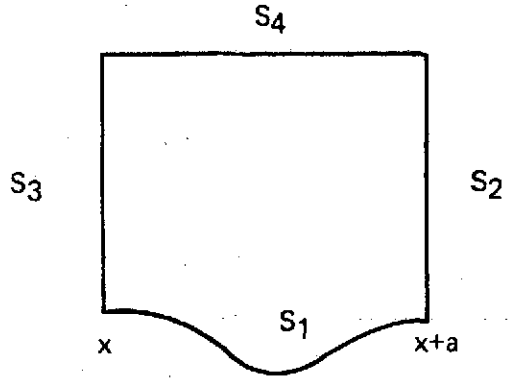

Fig. 1. Choice of surfaces of integration.

where $E_d(x',y')$ is the diffracted field, and if $E_i(x,y)$ is the incident field then the total electric field $E(x,y)$ is given by

$$E(x,y) = E_i(x,y) + E_d(x,y). \tag{6}$$

The integration is along the grating profile with the normal directed into the volume as shown in Fig. 2.

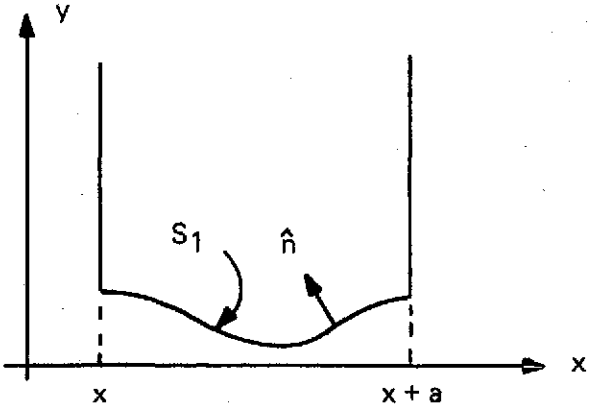

Fig. 2. The surface normal is directed into the volume enclosed by the surface used to evaluate the surface integral.

For the H-parallel polarization we obtain the result

$$H_d(x',y') = \exp(+ikx \sin\theta_i) \int_{S_1} \left[H(x,y) \frac{\partial G(x,y;x',y')}{\partial n} \right] dl. \tag{7}$$

As was the case with Eq. (5), H_d is the diffracted field, and the total field H is given by the sum of the incident field plus the diffracted fields

$$H(x,y) = H_i(x,y) + H_d(x,y). \tag{8}$$

In Eqs. (5) and (7) the elementary length (dl) for the contour integral along the grating profile may be converted to an integral along x by observing that

$$dl = \left[1 + \left(\frac{df(x)}{dx} \right)^2 \right]^{1/2} dx. \tag{9}$$

The limits of integration for the variable x are from $x = 0$ to $x = a$.

It is also useful to note that the normal derivative is given by

$$\frac{\partial}{\partial n} = \left[1 + \left(\frac{df(x)}{dx} \right)^2 \right]^{-1/2} \left[-\left(\frac{df(x)}{\partial x} \right) \frac{\partial}{\partial x} + \frac{\partial}{\partial y} \right]. \tag{10}$$

We may now write Eqs. (5) and (7) in a more convenient form by adding the respective incident fields to both sides and invoking the boundary conditions on the surface of the grating. For the E-parallel case we find that

$$E_i(x',f(x')) = + \exp(ikx' \sin\theta_i) \int_0^a G(x,f(x);x',f(x')) \left[1 + \left(\frac{df(x)}{dx} \right)^2 \right]^{1/2} \times \frac{\partial E(x,y)}{\partial n} \Bigg|_{y=f(x)} dx, \tag{11}$$

and for the H-parallel polarization we obtain

$$H_i(x',f(x')) = H(x',f(x')) - \exp(ikx' \sin\theta_i) \times \int_0^a \left\{ \frac{\partial G(x,y;x',y')}{\partial n} \left[1 + \left(\frac{df(x)}{dx} \right)^2 \right]^{1/2} H(x,y) \Bigg|_{\substack{y=f(x) \\ y'=f(x')}} \right\} dx \tag{12}$$

In Eqs. (11) and (12) the unknown quantities are $\partial E/\partial n$ and H. Thus, these two integral

equations can be solved for either $\partial E/\partial n$ or H on the surface of the grating. These quantities will be needed later in the analysis.

The Green's function $G(x,y;x',y')$ appearing in Eqs. (5) and (7) may be represented in various forms. The one form particularly suited to our needs is

$$G(x,y;x',y') = -\frac{\exp(-ikx\sin\theta_i)}{2ia}\sum_{m=-\infty}^{\infty}\frac{\exp[-i2\pi m(x-x')/a]\exp(+ik\cos\theta_m|y-y'|)}{k\cos\theta_m} \tag{13}$$

Also, the diffracted field can be represented as a discrete angular spectrum of plane waves

$$E_d(x',y') = \sum_{m=-\infty}^{\infty} A_m \exp[ik(x'\sin\theta_m + y'\cos\theta_m)]. \tag{14}$$

In both Eqs. (13) and (14) the index (m) labels the diffraction order. Equation (14) describes a plane wave whose wave normal makes an angle θ_m with the y axis and where the time dependence is given by the complex exponential $\exp(-i\omega t)$.

It is important to understand that the expansion coefficients A_m are constants (independent of x',y') only in the region away from the grooves of the grating. Inside the grooves they depend on both x' and y' as has been shown by Zaki and Kalhor. In the approximate theory of vector diffraction these coefficients were assumed to be constant everywhere.

We will use the expansion of Eq. (14) for E_d only in the region above the grating grooves. When Eqs. (13) and (14) are used in Eq. (5) we find the following expressions for the coefficients A_m

$$A_m = \left(\frac{-i}{2ak\cos\theta_m}\right)\int_0^a \exp[-ik(x\sin\theta_m + f(x)\cos\theta_m)]$$
$$\times\left[1+\left(\frac{df(x)}{dx}\right)^2\right]^{1/2}\frac{\partial E(x,y)}{\partial n}\bigg|_{y=f(x)}dx \tag{15}$$

for the E-parallel case. For the H-parallel case we obtain

$$B_m = \left(\frac{+i}{2ak\cos\theta_m}\right)\int_0^a H(x,y)\left[-\left(\frac{df(x)}{dx}\right)\frac{\partial}{\partial x}+\frac{\partial}{\partial y}\right]$$
$$\times\exp[-ik(x\sin\theta_m + y\cos\theta_m)]\bigg|_{y=f(x)}dx \tag{16}$$

where B_m is the expansion coefficient appearing in the discrete angular spectrum representation of H_d

$$H_d(x',y') = \sum_{m=-\infty}^{\infty} B_m \exp[ik(x' \sin\theta_m + y' \cos\theta_m)]. \tag{17}$$

In both Eqs. (15) and (16) the total fields E and H appear in the integrands. These are the values that these fields assume on the surface of the grating profile. The angular spectrum expansions with constant coefficients given in Eqs. (14) and (17) cannot be used for them. These fields may be found by solving the integral equations given in Eqs. (11) and (12) as mentioned previously.

In summary, the diffraction amplitudes A_m and B_m are obtained as follows. We first solve the integral equations given in Eqs. (11) and (12) to obtain the fields $\partial E/\partial n$ and H on the surface of the grating. These quantities are then used in Eqs. (15) and (16) to determine the amplitude coefficients A_m and B_m

3. MAXIMUM DIFFRACTION EFFICIENCY USING RIGOROUS DIFFRACTION THEORY

As reported in the 1971-1972 final report the problem of maximum diffraction efficiency was studied by using the computer programs based on the approximate theory. The amount of energy in a preassigned diffraction order was maximized by optimizing the initial solution. It was also shown that the values of θ_i and λ/a required to maximize the solution were the same conditions required to produce a double Wood's anomaly. We refer the reader to Fig. 5.3, p. 26, of that final report. We reproduce that curve here, in Fig. 3, for ease of reference. The plot shown in Fig. 3 is for the E-parallel state of polarization. However, the figure is not complete because the calculation was not performed for the H-parallel polarization. This is because the approximate theory was not able to produce reliable results for the H-parallel case. The calculation was later repeated using the Berkeley programs for both states of polarization. Below, in Fig. 4, we have reproduced the results of this calculation as they were first presented in the December 1972 monthly report. From Fig. 4 we see that

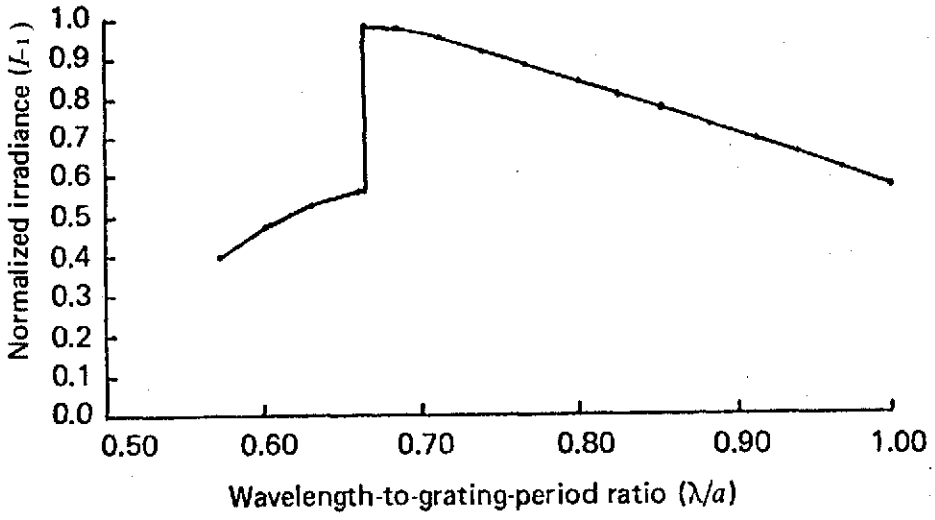

Fig. 3. Normalized irradiance λ/a for the -1st order versus the ratio λ/a for the E-parallel state of polarization. The angle of incidence is -19.47122.

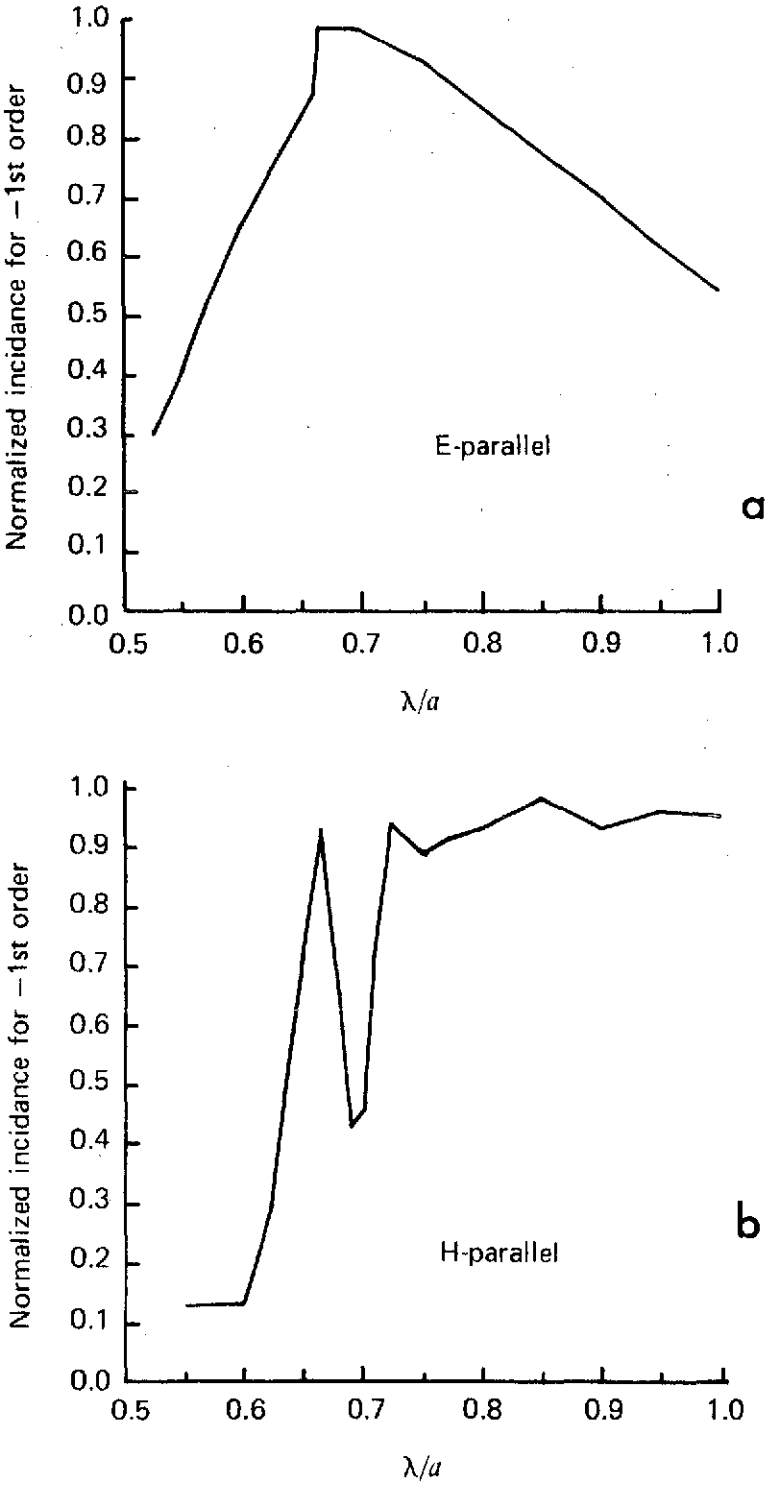

Fig. 4. Normalized irradiance for the −1st order versus λ/a for *E*-parallel (Fig. 4a) and *H*-parallel (Fig. 4b) states of polarization.

the calculation based on the rigorous theory corroborates the results obtained from the approximate theory for the E-parallel case. In Fig. 4b we see that the efficiency curve for the H-parallel case is a maximum at the same value of λ/a as was obtained for the E-parallel polarization. It is also apparent that the irradiance in the -1st order quickly drops to lower values on either side of the blaze condition $\lambda/a = 0.6667$ for the H-parallel case. Thus, we see that the grating is well blazed but only at a single wavelength.

The occurrence of high blaze efficiencies simultaneously with the phenomenon of double Wood's anomalies has also been reported by McPhedran.[3] In our studies this condition was obtained by optimizing the solution predicted by a geometrical model as reported in the monthly report dated 11 August 1972. At that time we reported on a graphical method for determining the grating parameters required to produce single and double Wood's anomalies. That method is presented below and we further show that the conditions required to produce a double Wood's anomaly are also the conditions necessary for one of the diffracted orders to be diffracted back along the direction of the incident beam. In fact, at the conditions that produce a double Wood's anomaly there is *always* one beam diffracted in the direction of the incident beam.

From the grating equation

$$\sin\theta_i + \sin\theta_m = \frac{m\lambda}{a}$$

where θ_i is the angle of incidence, θ_m is the diffraction angle for the mth order, m is the diffraction order, λ is the wavelength, and a is the grating constant, the ratio λ/a is solved for and plotted as a function of the angle of incidence for a given order m. The value of $\sin\theta_m$ is set equal to ± 1.0 because $\theta_m = \pm 90.0°$ when the mth order is evanescent. The curve so produced defines the values of λ, a, and θ_i required to produce a single Wood's anomaly. The intersection of two curves defines the conditions required to produce a double Wood's anomaly. Also, curves that lie above a given point on the graph indicate the real or homogeneous orders present for a given set of parameters. Curves below a given point represent inhomogeneous or evanescent orders. A plot showing the conditions required to produce single and double Wood's anomalies is shown in Fig. 5.

If we now take the grating equation and set $\theta_m = \theta_i$ and plot the ratio λ/a as a function of θ_i for a fixed order m, we obtain Fig. 6. These curves then give the conditions necessary for the mth order to be diffracted back along the direction of the incident beam. Under these conditions the mth order is in autocollimation (Littrow mount).

If we now superimpose Figs. 5 and 6 we obtain Fig. 7. This graph clearly shows that at the conditions required to produce a double Wood's anomaly there is always one diffraction order that is autocollimated. It is also apparent that there are more than one set of conditions for which a given order can be used in autocollimation in the presence of a double

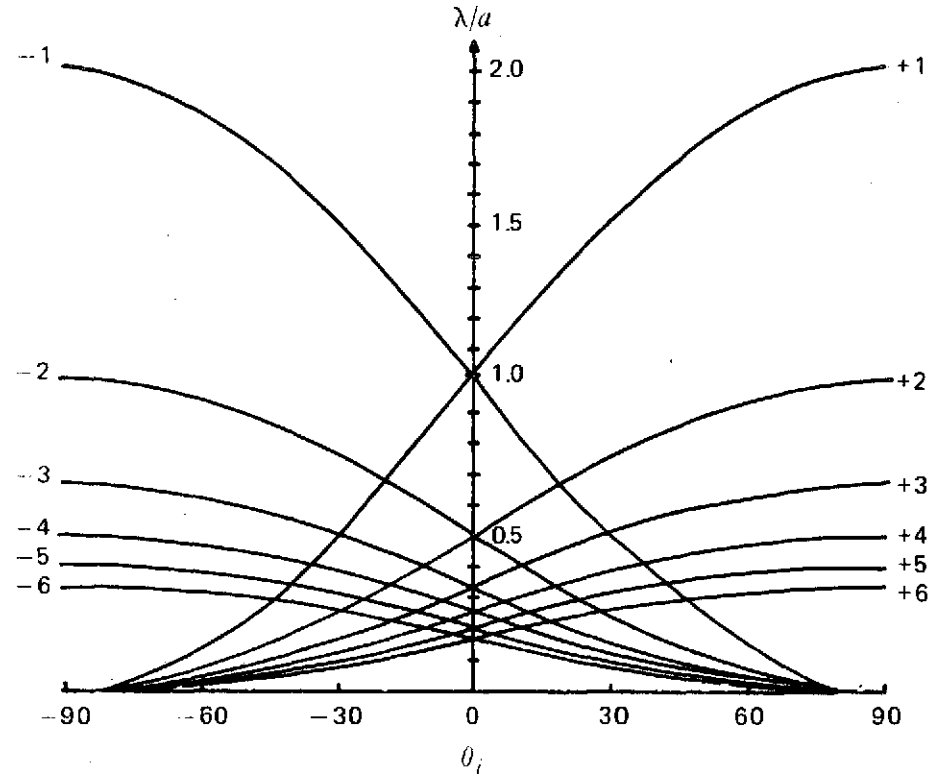

Fig. 5. Conditions for single and double Wood's anomalies.

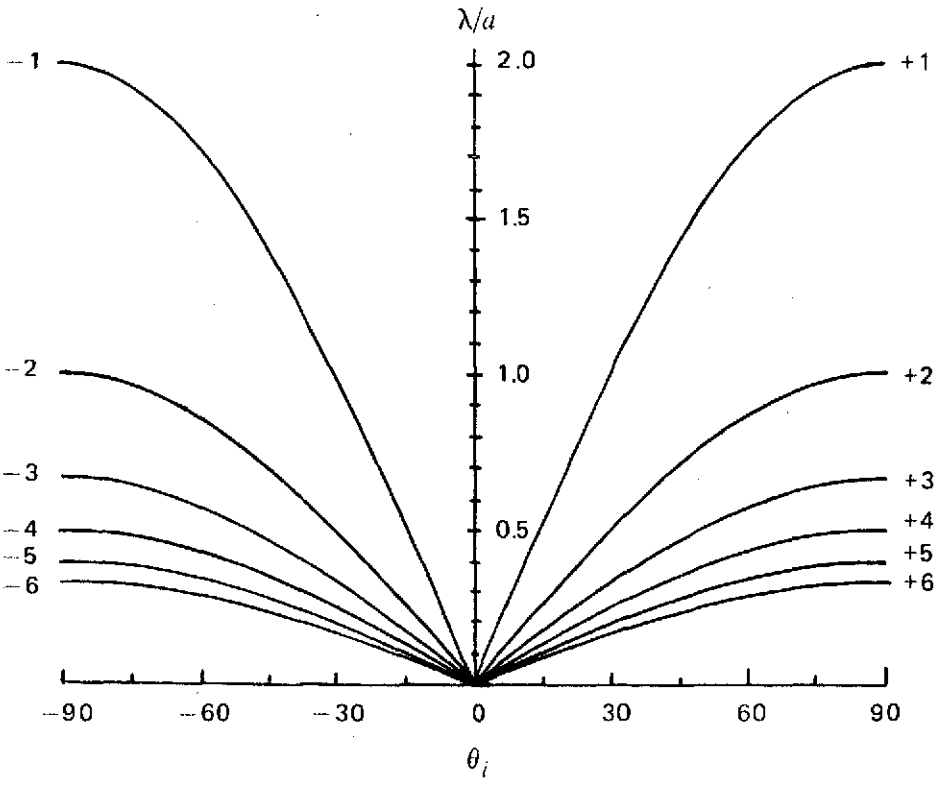

Fig. 6. Conditions required for autocollimation of mth order.

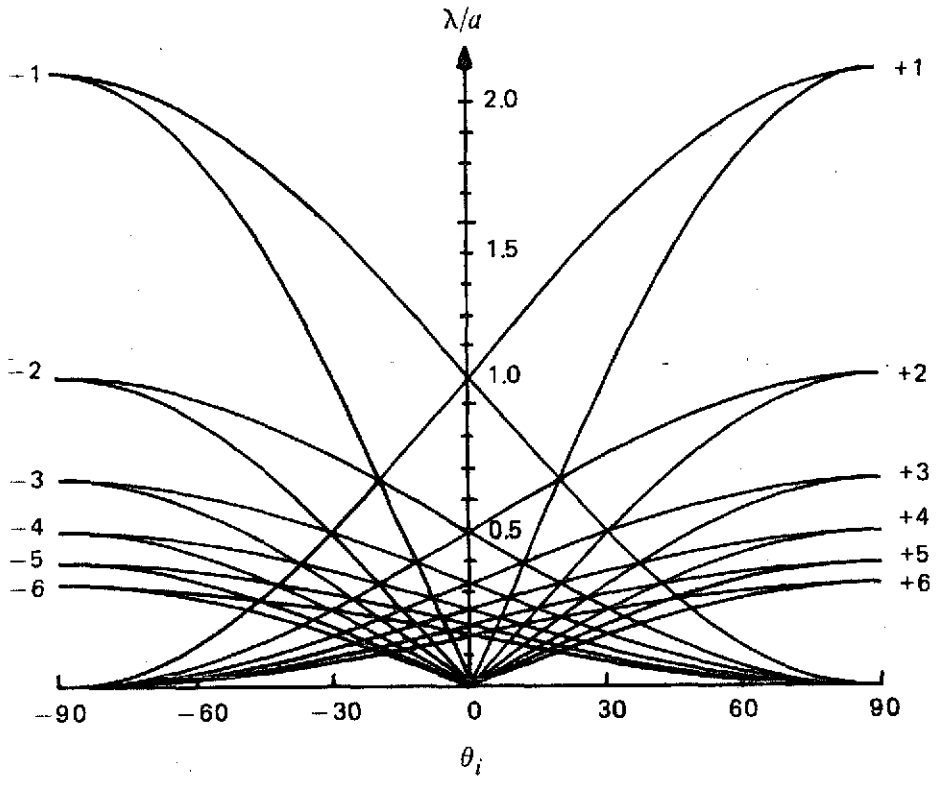

Fig. 7. Superposition of Figs. 5 and 6.

Wood's anomaly. From these graphs the conditions required to obtain a high blaze efficiency for a grating operated in the autocollimation mode can be easily obtained. We are currently preparing a paper for the *Journal of the Optical Society of America* reporting these findings.

4. MAXIMUM DIFFRACTION EFFICIENCY – AN ANALYTIC SOLUTION

The design of gratings that operate with a high blaze efficiency can also be persued analytically. This approach requires that the equations derived from vector diffraction theory be solved for the grating profile $f(x)$ that will produce the desired blazed conditions. This procedure would be extremely difficult to do using the equations derived from the rigorous theory. Thus, the equations obtained from the approximate theory are used, and the results are checked to insure that the $f(x)$ so obtained is consistent with the rigorous theory. In deriving the expression for the grating profile $f(x)$ we impose the constraint that all of the amplitude coefficients be exactly zero except one, the preselected blaze order denoted as the pth order. Thus,

$$A_m = \delta_{mp} \quad \text{for all } m. \tag{18}$$

The grating profile obtained from this study is given by

$$f(x) = -[p(\lambda/a)/2\cos\theta_i]x. \tag{19}$$

The blaze angle is given by

$$\alpha = \arctan[-p(\lambda/a)/2\cos\theta_i]. \tag{20}$$

The angle of incidence is

$$\theta_i = \arcsin[p/(\lambda/2a)], \tag{21}$$

and the apex angle ψ is given by

$$\psi = 90.0^\circ - \alpha. \tag{22}$$

This grating profile and the related parameters are shown in Fig. 8.

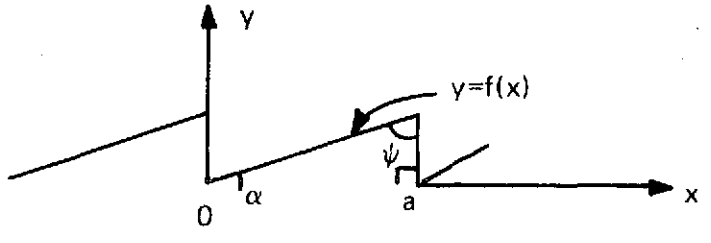

Fig. 8. Sketch of the profile $f(x)$ for maximum blaze efficiency as predicted by theory.

The predicted grating profile shown in Fig. 8 was tested using the computer programs based on the approximate theory. The results indicated that the profile produced a grating that was perfectly blazed (100%) for both states of polarization in a preselected diffraction order when the grating was used in autocollimation. Furthermore, the grating was blazed over a wavelength interval of approximately 18.0 nm. The groove depths used in the above study varied from less than one wavelength to 3.3 wavelengths. However, the energy check revealed that even for the deepest grating the computer programs based on the approximate theory were operating perfectly. This result suggests that the approximate theory had allowed us to predict a grating profile for which the amplitude coefficients were not a function of position within the grating grooves. This surprising result suggests that we (1) test the above profile with the Berkeley programs based on the exact theory and (2) investigate whether the above profile is also a solution of the exact equations when subjected to the same constraints.

In trying to test the above profile on the Berkeley programs we found that these programs would not run with the special profile and the constraint of autocollimation. However, by varying the angle of incidence slightly, the Berkeley programs would run. The energy check revealed that the rigorous programs were not operating as well as might be expected. Under these conditions the rigorous programs indicated that 92% of the incident energy was contained in the preselected order (the −4th order was chosen) for the *E* parallel state of polarization. It is believed that if the Berkeley programs had been able to operate under the ideal conditions, an energy check closer to unity would have been obtained together with more energy appearing in the desired order.

At this point we must mention that we have often encountered difficulty in getting the Berkeley programs to operate in a number of cases. Also, these programs and the approximate programs are not able to analyze some of the gratings in which NASA-GSFC has expressed interest. For these reasons we have embarked on a new method for obtaining a solution to the rigorous equations. In Section 5 of this report we describe these efforts in some detail.

We now focus our attention on the investigation of whether the profile $f(x)$ of Fig. 8 is also a solution of the exact equations. We start with the condition given in Eq. (18) and slightly modify it to read

$$A_m = \delta_{m,p} \qquad \text{all } m \text{ and } y \geq 0. \tag{23}$$

This modification sets a severe restriction on the behavior of the amplitude coefficients in the spaces above and within the grating grooves. It allows for no variation of A_m as a function of position within the grating grooves.

If the conditions expressed in Eq. (23) are used, then the diffracted fields can be expressed as an angular spectrum of plane waves with amplitude coefficients that are constant everywhere. The diffracted fields are therefore given by Eqs. (14) and (17). This means that

in the equations relating the amplitude coefficients A_m and B_m with the fields on the surface of the grating (Eqs. (15) and (16)) we may use the angular spectrum representation for the fields under the integral sign. Under these conditions the rigorous equations become much simpler, and we have shown (see Appendix A) that the special grating profile given by Eq. (19) is also predicted by the equations of the exact theory. We intend to publish these findings in the *Journal of the Optical Society of America.*

5. A NEW METHOD FOR THE SOLUTION OF THE RIGOROUS THEORY EQUATIONS

One of the gratings that NASA-GSFC has expressed an interest in is the coarse echelle grating used in the vacuum ultraviolet. In general, these gratings tend to be very deep with respect to the wavelength of the radiant energy. Also, it is not uncommon for more than 100 real diffraction orders to be present for a coarse echelle as opposed to only a few real orders as is usually the case for an echelette grating. As a result, it is not possible to analyze coarse echelle gratings by using existing computer programs. In addition, it is not possible to simply increase the number of diffraction orders that current programs can analyze because the programs soon become too large for the computer (CDC 6400). Thus, a new method of analysis must be formulated for echelle gratings. Below we outline a new approach for calculating the amplitude coefficients by using rigorous vector diffraction theory. For this method we hope to obtain a more convenient set of equations that can even be used when there are a large number of orders present. In Appendices B, C, and D a mathematical description of important parameters can be found.

Before discussing the method of solution, we want to point out some of the difficulties to be expected in applying the rigorous vector diffraction equations to the study of echelle gratings.

First, a computer can perform operations only on discrete or sampled values of a function. The number of sampled values required to adequately represent a given function depends on how quickly the function varies: slowly varying functions require fewer sampled values than rapidly varying functions. Therefore, a function of two independent variables, $k(x,x')$, may require a very large two-dimensional matrix to store all of the sampled values required to represent $k(x,x')$ if the function is rapidly varying.

In the echelle problem for the E-parallel polarization, we wish to solve Eq. (11) for the unknown quantity $\partial E(x,f(x))/\partial n$. This quantity (matrix of sampled values) is then used in Eq. (15) to calculate the unknown amplitude coefficients for the diffracted fields. In order to solve Eq. (11) for the unknown quantity $\partial E(x,f(x))/\partial n$ we must first calculate the elements of the matrix representing the Green's function $G(x,f(x);\ x',f(x'))$ as given by Eq. (13). However, in Eq. (13) the index m is the diffraction order and appears in one of the exponentials. For large values of m (up to 100) this exponential will be a rapidly oscillating function and, therefore, the Green's function will require a very large matrix to contain all of the necessary sampled values. A simple calculation shows that for 100 real orders the size of this matrix alone exceeds the available core storage of many large computers.

One way of overcoming the above storage requirement is to express the Green's function in terms of functions that are more slowly varying than the plane wave representation Eq. (13). Another possible representation for the Green's function is in terms of Hankel functions. This representation converges rapidly for gratings with a period much greater than the

wavelength of the radiant energy. This condition is easily met with coarse echelle gratings but not necessarily with echelette and holographic gratings. Therefore, the Hankel function representation is of limited use in our work.

It is not unusual for functions that are rapidly varying in the spatial domain to be much smoother in the spatial frequency domain. For such functions the analysis can be performed in the frequency domain by using smaller matrices. In the work presented below we have chosen to perform the calculations in the frequency domain with the aim of reducing the sizes of the required matrices. This is done by expressing all of the quantities in terms of their complex Fourier series expansions. This method has an additional benefit due to the uniqueness of the Fourier series. Namely, that the plane wave and the Hankel function representations of the Green's function (as well as any other representations) must have the same Fourier representation. This means that the Fourier method can be used for the analysis of echelettes as well as coarse echelle gratings if the matrices are of reasonable dimensions in the case of the latter.

To illustrate the proposed method of analysis we note that Eq. (11) is of the form

$$h(x') = \int_0^a k(x,x')g(x)dx, \tag{24}$$

where

$$\begin{aligned} h(x') &\equiv E_i(x',f(x')) \\ k(x,x') &\equiv i \exp(+ikx' \sin\theta_i)G(x,f(x);x',f(x')) \\ g(x) &\equiv (\ \ i)\left[1+\left(\frac{df(x)}{dx}\right)^2\right]^{1/2} \frac{\partial E(x,f(x))}{\partial n} \end{aligned} \tag{25}$$

and

$$E(x,f(x)) = E_i(x,f(x)) + E_d(x,f(x)).$$

We then expand each of these functions in terms of their Fourier series representations

$$\begin{aligned} h(x') &\equiv \sum_{k=-\infty}^{\infty} h_k \exp(+i2\pi kx'/a) \\ k(x,x') &\equiv \sum_{n=-\infty}^{\infty} \sum_{j=-\infty}^{\infty} k_{j,n} \exp(-i2\pi nx/a) \exp(+i2\pi jx'/a) \\ g(x) &\equiv \sum_{l=-\infty}^{\infty} g_l \exp(+i2\pi lx/a). \end{aligned} \tag{26}$$

The complex expansion coefficients are then given by

$$h_k = \frac{1}{a}\int_0^a h(x')\exp(-i2\pi kx'/a)dx'$$

$$k_{j,n} = \frac{1}{a^2}\int_0^a\int_0^a k(x,x')\exp(+i2\pi nx/a)\exp(-i2\pi jx'/a)dxdx' \tag{27}$$

$$g_l = \frac{1}{a}\int_0^a g(x)\exp(-i2\pi lx/a)dx.$$

Substitution of Eq. (26) into Eq. (24) yields

$$\sum_{k=-\infty}^{\infty} h_k \exp(+i2\pi kx'/a) = \int_0^a \sum_{n=-\infty}^{\infty}\sum_{j=-\infty}^{\infty} k_{j,n}\exp(-i2\pi nx/a)$$

$$\times \exp(+i2\pi jx'/a)\sum_{l=-\infty}^{\infty} g_l \exp(+i2\pi lx/a)dx. \tag{28}$$

After some manipulation Eq. (28) becomes

$$\sum_{k=-\infty}^{\infty}(h_k)\exp(+i2\pi kx'/a) = \sum_{j=-\infty}^{\infty}\left(a\sum_{n=-\infty}^{\infty}k_{j,n}g_n\right)\exp(+i2\pi jx'/a). \tag{29}$$

For Eq. (29) to be valid for all terms in the expansion we must have

$$\sum_{j=-\infty}^{\infty}(h_j)\exp(+i2\pi jx'/a) = \sum_{j=-\infty}^{\infty}\left(a\sum_{n=-\infty}^{\infty}k_{j,n}g_n\right)\exp(+i2\pi jx'/a)$$

or

$$h_j = a\sum_{n=-\infty}^{\infty}k_{j,n}g_n. \tag{30}$$

Equation (30) is a matrix equation where h and g are column matrices and k is a two-dimensional matrix. The size of the matrices is determined by the values of j and n beyond

which the contributions of the series for h and k are less than the specified error. That is, n and j cannot assume the infinite limits expressed above but must be limited to some maximum value. The maximum values are chosen such that the errors due to neglecting terms beyond these maximum values are less than a specified amount.

We wish to determine the unknown expansion coefficient g_n in Eq. (30). This can be done because we can calculate the coefficients h_j and $k_{j,n}$ because they involve known quantities. In Appendix B we have derived the equations from which the $k_{j,n}$ coefficients are to be calculated. In Appendix C we derive the equations for the coefficients h_j.

Note that j and n can assume negative as well as positive values. If we denote the minimum values as *JMIN* and *NMIN* and the maximum values as *JMAX* and *NMAX* then the number of values that j and n will assume are given by J and N, respectively, where,

$$J \equiv JMAX - JMIN + 1$$

$$N \equiv NMAX - NMIN + 1. \tag{31}$$

In general, we will have $J = N$. This means that we can regard Eq. (30) as either a matrix equation or as N simultaneous equations. Solution of the matrix equation will require that the inverse matrix $k^{-1}_{j,n}$ be calculated. In any case, once the coefficients g_n are solved for the function, $g(x)$ is determined. Note that $g(x)$, as defined in Eq. (25), also appears as the unknown in the equation for the amplitude coefficients Eq. (15), namely,

$$A_m = \left(\frac{1}{2ak\cos\theta_m}\right)\int_0^a \exp[-ik(x\sin\theta_m + f(x)\cos\theta_m]g(x)dx. \tag{32}$$

We now expand the complex exponential in terms of its Fourier series representation

$$e_m(x) \equiv \exp[-ik(x\sin\theta_m + f(x)\cos\theta_m)] = \sum_{n=-\infty}^{\infty} e_{m,n}\exp(-i2\pi nx/a). \tag{33}$$

Thus,

$$A_m = \left(\frac{1}{2ak\cos\theta_m}\right)\int_0^a \sum_{n=-\infty}^{\infty} e_{m,n}\exp(-i2\pi nx/a)\sum_{l=-\infty}^{\infty} g_l\exp(+i2\pi lx/a)dx$$

$$= \left(\frac{1}{2ak\cos\theta_m}\right)\sum_{n=-\infty}^{\infty}\sum_{l=-\infty}^{\infty} e_{m,n}g_l a\delta_{l,n}$$

$$A_m = \left(\frac{1}{2k\cos\theta_m}\right) \sum_{n=-\infty}^{\infty} e_{m,n} g_n . \tag{34}$$

Equation (34) is also a matrix equation where A and g are column matrices and $e_{m,n}$ is a two-dimensional matrix. The coefficients $e_{m,n}$ are to be calculated from

$$e_{m,n} = \frac{1}{a}\int_0^a e_m(x)\exp(+i2\pi nx/a)dx. \tag{35}$$

Explicit expressions for the $e_{m,n}$ coefficients are derived in Appendix D. Once these coefficients have been calculated we can then calculate the unknown amplitude coefficients A_m using simple matrix multiplication.

We note that the method of analysis is the same for the H-parallel state of polarization except that $g(x)$ would now be proportional to the magnetic field and $k(x,x')$ would represent the normal derivative of the Green's function.

APPENDIX A

CONSISTENCY OF SPECIAL BLAZED GRATING PROFILE WITH EQUATIONS DERIVED FROM THE RIGOROUS THEORY

The amplitude coefficients for each of the diffracted orders are given by

$$A_m = \left(\frac{-i}{2ak\cos\theta_m}\right)\int_0^a \exp[-ik(x\sin\theta_m + f(x)\cos\theta_m)]$$

$$\times\left[1+\left(\frac{df(x)}{dx}\right)^2\right]^{1/2}\frac{\partial E(x,f(x))}{\partial n}\,dx. \tag{A1}$$

We assume a plane wave expansion for the diffracted fields of the form

$$E_d(x,y) = \sum_{m=-\infty}^{\infty} A_m \exp[ik(x\sin\theta_m + y\cos\theta_m)]. \tag{A2}$$

We also note that

$$\frac{\partial}{\partial n} = \left[-\left(\frac{df(x)}{dx}\right)\frac{\partial}{\partial x} + \frac{\partial}{\partial y}\right]\left[1+\left(\frac{df(x)}{dx}\right)^2\right]^{-1/2}. \tag{A3}$$

If we use Eq. (A3) to operate on the total electric field and we substitute into Eq. (A1), we obtain after considerable manipulation

$$-\int_0^a \left(\frac{df(x)}{dx}\sin\theta_i + \cos\theta_i\right)\exp[-ikf(x)(\cos\theta_n + \cos\theta_i)]\exp(-i2\pi nx/a)dx$$

$$= \sum_{m=-\infty}^{\infty} A_m \left\{\int_0^a \left(\frac{df(x)}{dx}\sin\theta_m - \cos\theta_m\right)\exp[-ikf(x)(\cos\theta_n - \cos\theta_m)]\right.$$

$$\left.\times\exp[-i2\pi(n-m)x/a]dx + 2a\cos\theta_m\delta_{mn}\right\}. \tag{A4}$$

In deriving the equation of the grating profile we imposed the constraints

$$A_m = \delta_{mp}, \qquad \text{for all } m$$
$$\theta_m = \theta_i. \tag{A5}$$

These constraints are then used to simplify Eq. (A4). The left-hand side (LHS) of the equation then becomes

$$\text{LHS} = -\sin\theta_i \int_0^a \frac{df(x)}{dx} \exp(-i2kf(x)\cos\theta_i - i2\pi px/a)dx$$

$$-\cos\theta_i \int_0^a \exp(-i2kf(x)\cos\theta_i - i2\pi px/a)dx. \tag{A6}$$

The right-hand side (RHS) reduces to

$$\text{RHS} = f(a)\sin\theta_i + a\cos\theta_i. \tag{A7}$$

When we match coefficients for $\sin\theta_i$ in Eqs. (A6) and (A7) we obtain

$$f(a) = -\int_0^a \frac{df(x)}{dx} \exp(-i2kf(x)\cos\theta_i - i2\pi px/a)dx. \tag{A8}$$

The grating profile $f(x)$ is given by

$$f(x) = -\left(\frac{p(\lambda/a)}{2\cos\theta_i}\right)x. \tag{A9}$$

Substitution of Eq. (A9) into Eq. (A8) for the value $x = a$ yields the identity $f(a) = f(a)$. Thus we see that Eq. (A9) is a solution of the rigorous equations under the constraints expressed by Eqs. (A2) and (A5).

APPENDIX B

EXPANSION COEFFICIENTS $k_{j,n}$

In Section 5 of the text we defined

$$k(x,x') \equiv i \exp[+ikx' \sin\theta_i] G(x,f(x); x',f(x')) \tag{B1}$$

where $G(x,f(x); x',f(x'))$ is the Green's function given by

$$G(x,f(x); x',f(x')) = -\frac{\exp(+ikx \sin\theta_i)}{2ia} \times \sum_{m=-\infty}^{\infty} \frac{\exp[-i2\pi m(x - x')/a] \exp(+ik \cos\theta_m |f(x) - f(x')|]}{k \cos\theta_m} . \tag{B2}$$

Recall that we expressed $k(x,x')$ in terms of its Fourier series expansion

$$k(x,x') = \sum_{n=-\infty}^{\infty} \sum_{j=-\infty}^{\infty} k_{j,n} \exp(-i2\pi nx/a) \exp(+i2\pi jx'/a). \tag{B3}$$

Therefore, the expansion coefficients are given by

$$k_{j,n} = \frac{1}{a^2} \int_0^a \int_0^a k(x,x') \exp(+i2\pi nx/a) \exp(-i2\pi jx'/a) dx dx'. \tag{B4}$$

In order for these coefficients to be calculated we insert Eq. (B2) into Eq. (B1) and the resulting expression is used in Eq. (B4).

In order for the calculation to be completed we must know the equation of the grating profile $f(x)$.

For this derivation we assume $f(x)$ to be the profile shown in Fig. B1. The actual grating profile is given by

$$f(x) = \begin{cases} Ax, & 0 \leq x \leq x_1 \\ \dfrac{Ax_1}{a - x_1} (a - x), & x_1 \leq x \leq a \end{cases} \tag{B5}$$

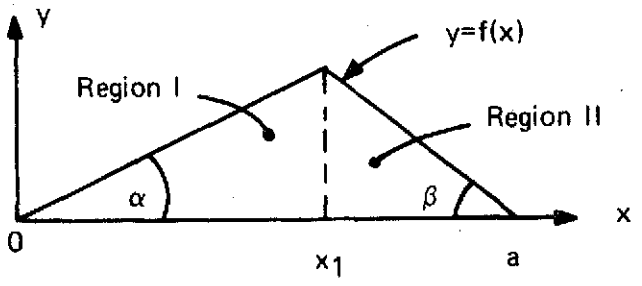

Fig. B1. Grating profile $f(x)$.

where A is the slope of $f(x)$ in Region I ($A = \tan\alpha$). After much calculation we find the expression on page 26 for the Fourier expansion coefficients $k_{j,n}$ for the profile shown in Fig. B1.

$$K_{j,n}=\sum_{m=-\infty}^{\infty}(C_m/4\pi^2)\Bigg(\left(\frac{P_{12}^{(m)}}{a-jP_{12}^{(m)}}\right)\left\{\frac{e^{+i2\pi(n-j)x_1/a}-e^{+i2\pi(1/P_{12}^{(m)}-j/a)x_1}}{(a-nP_{12}^{(m)})/P_{12}^{(m)}}\right.$$

$$-\left(\frac{P_{11}^{(m)}}{a-jP_{11}^{(m)}}\right)\left\{\frac{e^{-i2\pi(1/P_{11}^{(m)}-n/a)x_1}-1}{(a-nP_{11}^{(m)})/P_{11}^{(m)}}+\frac{e^{+i2\pi(n-j)x_1/a}-1}{(n-j)}\right\}$$

$$+\frac{e^{-ikBaCos\theta_m}}{a}\left(\frac{P_{22}^{(m)}}{a-jP_{22}^{(m)}}\right)\left\{\frac{e^{+i2\pi(a/P_{22}^{(m)}-j)}(e^{-i2\pi\gamma_1x_1}-1)}{\gamma_1}\right.$$

$$\left.-\left(\frac{aP_{12}^{(m)}}{a-nP_{12}^{(m)}}\right)e^{+i2\pi(1/P_{22}^{(m)}-j/a)x_1}\left(e^{-i2\pi(1/P_{12}^{(m)}-n/a)x_1}-1\right)\right\}$$

$$+\frac{e^{+ikBaCos\theta_m}}{a}\left(\frac{P_{21}^{(m)}}{a-jP_{21}^{(m)}}\right)\left\{\left(\frac{aP_{11}^{(m)}}{a-nP_{11}^{(m)}}\right)e^{+i2\pi(1/P_{12}^{(m)}-j/a)a}\right.$$

$$\left.\times\left(e^{-i2\pi(1/P_{11}^{(m)}-n/a)x_1}-1\right)-\frac{e^{+i2\pi(a/P_{21}^{(m)}-j)}(e^{-i2\pi\gamma_2x_1}-1)}{\gamma_2}\right\}$$

$$+\left(\frac{P_{11}^{(m)}e^{-ikBaCos\theta_m}}{a(a-jP_{11}^{(m)})}\right)\left\{\left(\frac{e^{-i2\pi\gamma_3a}-e^{-i2\pi\gamma_3x_1}}{\gamma_3}\right)e^{+i2\pi(a/P_{11}^{(m)}-j)x_1/(a-x_1)}\right.$$

$$\left.-\left(\frac{aP_{21}^{(m)}}{a-nP_{21}^{(m)}}\right)\left(e^{-i2\pi(a/P_{21}^{(m)}-n)}-e^{-i2\pi(1/P_{21}^{(m)}-n/a)x_1}\right)\right\}$$

$$+\left(\frac{P_{12}^{(m)}e^{+ikBaCos\theta_m}}{a(a-jP_{12}^{(m)})}\right)\left\{\left(\frac{aP_{22}^{(m)}}{a-nP_{22}^{(m)}}\right)\left(e^{-i2\pi(a/P_{22}^{(m)}-n)}-e^{-i2\pi(1/P_{22}^{(m)}-n/a)x_1}\right)\right.$$

$$\left.\times e^{+i2\pi(1/P_{12}^{(m)}-j/a)x_1}-\frac{e^{+i2\pi(a/P_{12}^{(m)}-j)x_1/(a-x_1)}(e^{-i2\pi\gamma_4a}-e^{-i2\pi\gamma_4x_1})}{\gamma_4}\right\}$$

$$+\left(\frac{P_{22}^{(m)}}{a-jP_{22}^{(m)}}\right)\left\{\left(\frac{1-e^{-i2\pi(j-n)x_1/a}}{j-n}\right)-\left(\frac{P_{22}^{(m)}}{a-nP_{22}^{(m)}}\right)\left(e^{+i2\pi\gamma_5}-e^{-i2\pi(n-j)x_1/a}\right)\right\}$$

$$+\left(\frac{P_{21}^{(m)}}{a-jP_{21}^{(m)}}\right)\left\{\left(\frac{P_{21}^{(m)}}{a-nP_{21}^{(m)}}\right)(1-e^{+i2\pi\gamma_6})+\left(\frac{1-e^{+i2\pi(n-j)x_1/a}}{n-j}\right)\right\}\Bigg)$$

where,

$$\gamma_1 \equiv \left(\frac{1}{P_{12}^{(m)}} - \frac{n}{a} - \frac{1}{P_{22}^{(m)}} + \frac{j}{a} + \frac{a}{x_1 P_{22}^{(m)}} - \frac{j}{x_1} \right)$$

$$\gamma_2 \equiv \left(\frac{1}{P_{11}^{(m)}} - \frac{n}{a} - \frac{1}{P_{21}^{(m)}} + \frac{j}{a} + \frac{a}{x_1 P_{21}^{(m)}} - \frac{j}{x_1} \right)$$

$$\gamma_3 \equiv \left(\frac{1}{P_{21}^{(m)}} - \frac{n}{a} + \frac{x_1}{P_{11}^{(m)}(a-x_1)} - \frac{jx_1}{a(a-x_1)} \right)$$

$$\gamma_4 \equiv \left(\frac{1}{P_{22}^{(m)}} - \frac{n}{a} + \frac{x_1}{P_{21}^{(m)}(a-x_1)} - \frac{jx_1}{a(a-x_1)} \right)$$

$$\gamma_5 \equiv \left(\frac{x_1}{P_{22}^{(m)}} - \frac{jx_1}{a} - \frac{a}{P_{22}^{(m)}} + n \right)$$

$$\gamma_6 \equiv \left(\frac{a}{P_{21}^{(m)}} + \frac{nx_1}{a} - \frac{x_1}{P_{21}^{(m)}} - j \right)$$

$$P_{11}^{(m)} \equiv \left(\frac{\mathrm{Sin}\theta_i}{\lambda} + \frac{m}{a} - \frac{A\mathrm{Cos}\theta_m}{\lambda} \right)^{-1}$$

$$P_{12}^{(m)} \equiv \left(\frac{\mathrm{Sin}\theta_i}{\lambda} + \frac{m}{a} + \frac{A\mathrm{Cos}\theta_m}{\lambda} \right)^{-1}$$

$$P_{21}^{(m)} \equiv \left(\frac{\mathrm{Sin}\theta_i}{\lambda} + \frac{m}{a} - \frac{B\mathrm{Cos}\theta_m}{\lambda} \right)^{-1}$$

$$P_{22}^{(m)} \equiv \left(\frac{\mathrm{Sin}\theta_i}{\lambda} + \frac{m}{a} + \frac{B\mathrm{Cos}\theta_m}{\lambda} \right)^{-1}$$

$A \equiv \mathrm{Tan}\,\alpha$, $B \equiv -\mathrm{Tan}\,\beta$.

APPENDIX C

EXPANSION COEFFICIENTS h_j

Using Eq. (27) of the text for the expansion coefficients h_j we have

$$h_j = \frac{1}{a}\int_0^a h(x')\exp[-i2\pi jx'/a]\,dx' \tag{C1}$$

where $h(x')$ is the incident electric field

$$h(x') \equiv \exp[-ikx'\sin\theta_i]\exp[-ikf(x')\cos\theta_i]. \tag{C2}$$

We use the same grating profile $f(x')$ defined in Eq. (B5) of Appendix B. In this way we find the following expression for the Fourier expansion coefficients

$$h_j = \left(\frac{i}{2\pi a}\right)\left\{\frac{1}{\alpha}\left[\exp(-i2\pi\alpha x_1) - 1\right] + \left(\frac{1}{\beta}\right)\exp(-ikBa\cos\theta_i)\right.$$

$$\left.\times\left[\exp(-i2\pi\beta a) - \exp(-i2\pi\beta x_1)\right]\right\} \tag{C3}$$

where

$$\alpha \equiv (\sin\theta_i/\lambda + A\cos\theta_i/\lambda + j/a)$$

$$\beta \equiv (\sin\theta_i/\lambda - B\cos\theta_i/\lambda + j/a).$$

APPENDIX D

EXPANSION COEFFICIENTS $e_{m,n}$

Using Eq. (35) of the text for the expansion coefficients $e_{m,n}$ we have

$$e_{m,n} = \frac{1}{a}\int_0^a e_m(x)\exp(+i2\pi nx/a]\,dx \tag{D1}$$

where

$$e_m(x) \equiv \exp[-ik(x\sin\theta_m + f(x)\cos\theta_m)]. \tag{D2}$$

We use the same grating profile $f(x)$ defined in Eq. (B5) of Appendix B. In this way we obtain the following expression for the Fourier expansion coefficients

$$e_{m,n} = \left(\frac{i}{2\pi a}\right)\left\{\left(\frac{1}{\alpha}\right)[\exp(-i2\pi\alpha x_1) - 1] + \exp(-i2\pi Ba\cos\theta_m)\left(\frac{1}{\beta}\right)\right.$$
$$\left.\times\,[\exp(-i2\pi\beta a) - \exp(-i2\pi\beta x_1)]\right\} \tag{D3}$$

where

$$\alpha \equiv (\sin\theta_m/\lambda + A\cos\theta_m/\lambda - n/a)$$

$$\beta \equiv (\sin\theta_m/\lambda - B\cos\theta_m/\lambda - n/a).$$

REFERENCES

1. Zaki, K. A. E. H., "Numerical methods for the analysis of scattering from nonplanar periodic structures," Dissertation, University of California at Berkeley, 1969.
2. Kalhor, H. A., "Numerical integral-equation analysis of scattering from diffraction gratings," Dissertation, University of California at Berkeley, 1970.
3. McPhedran, R. C., and M. D. Waterworth, "Blaze optimization for triangular profile gratings," Optica Acta 20:3, 1973.